Saudi Journal of Biological Sciences 28 (2021) 2301–2315

Contents lists available at ScienceDirect

Saudi Journal of Biological Sciences

journal homepage: www.sciencedirect.com

Original article

Molecular characterization of *Leucoanthocyanidin reductase* and *Flavonol synthase* gene in *Arachis hypogaea*

Ghulam Kubra [a], Maryam Khan [a], Sidra Hussain [a], Tooba Iqbal [a], Jan Muhammad [a], Hina Ali [b], Alvina Gul [a], Faiza Munir [a], Rabia Amir [a,*]

[a] *Atta-ur-Rahman School of Applied Biosciences (ASAB), National University of Sciences and Technology (NUST), Islamabad 44000, Pakistan*
[b] *National Institute for Lasers and Optronics (NILOP), Lehtrar Road, Islamabad 44000, Pakistan*

ARTICLE INFO

Article history:
Received 2 November 2020
Revised 6 January 2021
Accepted 10 January 2021
Available online 23 January 2021

Keywords:
Arachis hypogaea
Flavonoids
Flavonol synthase
Leucoanthocyanidin reductase
Characterization

ABSTRACT

Arachis hypogaea (peanut) is a potential source of bioactive compounds including flavonols and proanthocyanidins, which have gained particular interest of metabolic engineering owing to their significance in the growth, development and defense responses in plants. To gain insight of proanthocyanidins and flavonols production in *A. hypogaea*, *Leucoanthocyanidin reductase (AhLAR)* and *Flavonol synthase (AhFLS)* enzymes responsible for their production, have been structurally, transcriptionally and functionally characterized. Structural and functional analysis of putative protein sequence of *AhFLS* indicated two functional motifs 2OG-FeII_Oxy and DIOX_N, while six functional motifs belonging to the families of NAD-dependent dehydratase, 3, *β hydroxysteroid dehydrogenase* and NmrA-like family were observed in case of *AhLAR*. Promoter sequence analysis unraveled several promoter elements related to the development regulation, environmental stress responses and hormonal signaling. Furthermore, the expression analysis of *AhFLS* and *AhLAR* and accumulation pattern analysis of proanthocyanidins and flavonols in three selected cultivars of *A. hypogaea* under saline environment confirmed their role against salinity in genotype-dependent and stress level-dependent manner. Correlation studies revealed that AhFLS and AhLAR expression is not directly dependent on the antioxidant enzymes activity, biochemical and growth parameters but higher Pearson r value depicted some level of dependency. This detailed study of AhLAR and AhFLS can assist in the metabolic engineering of flavonoid biosynthetic pathway to produce stress tolerant varieties and production of proanthocyanidins and flavonols at an industrial scale.

1. Introduction

Flavonoids are phenolic secondary metabolites that perform diverse array of metabolic functions in higher plants (Saito et al., 2013). Owing to their structural diversity, most of the flavonoids exhibit biological activity in the field of organic synthesis, natural product chemistry, food chemistry, medicinal chemistry, biology, toxicology, and biochemistry (Rauter et al., 2018). Plants produce flavonoids as oviposition stimulants, visual attractors, phytoalexins, allelopathy, antimicrobials, feeding repellents, photoreceptors, and antioxidants (Nabavi et al., 2020). However, these functions are not well conserved within plant species (Pelletier et al., 1997).

Flavonoids are widely distributed in Kingdom Plantae and their biosynthetic pathway has been explored extensively, both molecularly and biochemically (Yonekura-Sakakibara et al., 2019). During evolution, flavonoids have diversified from its original functions i.e., regulation of phytohormone and UV irradiation (Rausher et al., 1999). Consequently, developing metabolic pathways that assist in acquiring diversity in specialized metabolites (Yonekura-Sakakibara et al., 2019). Mostly, the enzymes involved in secondary metabolism are derived from primary metabolism e.g., early pathway enzymes of flavonoid biosynthetic pathway, *Chalcone synthase*

Abbreviations: AhLAR, Leucoanthocyanidin reductase; AhFLS, Flavonol synthase; CHS, Chalcone synthase; CHI, Chalcone isomerase; SDR, short-chain dehydrogenase/reductase; ROS, reactive oxygen species; SOD, superoxide dismutase; CAT, catalase; APX, ascorbate peroxidase; Ab, absorbance; EC, extinction coefficient; CDS, coding sequences; CDD, Conserved Domain Database; ANOVA, Analysis of variance; ORF, open reading frame.

* Corresponding author.
E-mail addresses: rabi.amir@hotmail.com, rabia@asab.nust.edu.pk (R. Amir).

Peer review under responsibility of King Saud University.

Production and hosting by Elsevier

https://doi.org/10.1016/j.sjbs.2021.01.024
1319-562X/

(CHS) and *Chalcone isomerase* (CHI), originated from fatty acid metabolism. However, the late pathway enzymes include members from superfamilies of short-chain dehydrogenase/reductase (SDR), CYP and 2OGD evolved as a result of gene duplication (Ngaki et al., 2012; Yonekura-Sakakibara et al., 2019).

The early pathway genes happen to be regulated in coordination, whereas the late pathway genes such as *Flavonol synthase* (FLS) and *Leucoanthocyanidin reductase* (LAR) exhibit a distinctive expression pattern in a species or tissue specific manner. FLS and LAR belong to two distinct branches of flavonoid biosynthetic pathway and lead to the production of flavonols and proanthocyanidins, respectively (Nabavi et al., 2018; Zhang et al., 2020). Both enzymes are of particular interest in the field of metabolic engineering, owing to the significance of their products. Additionally, flavonols and proanthocyanidins have imperative role in the defense response against both biotic and abiotic stress in plants due to their free radical scavenging and antioxidant activity (Andersen and Markham, 2005; Muhlemann et al., 2018).

Oxidative stress generated by reactive oxygen species (ROS) initiates flavonoid biosynthesis, since severe stress conditions hinder the activity of antioxidant enzymes such as superoxide dismutase (SOD), catalase (CAT) and ascorbate peroxidase (APX) (Nabavi et al., 2020). Flavonols and proanthocyanidins are naturally occurring antioxidants that not only scavenge ROS but also inhibit their production (Jia et al., 2012; Martinez et al., 2016). Various studies have suggested that flavonoids establish a secondary ROS scavenging system because profuse excitation energy is being directed to photosynthesis due to severe oxidative stress, however, these studies are not conclusive (Martinez et al., 2016).

The presented study is designed to gain insight of genetic and functional diversity of *AhFLS* and *AhLAR* in *Arachis hypogaea* (Peanut) that harbors a plethora of diverse secondary metabolites. *Insilico* functional analysis has been performed on *AhFLS* and *AhLAR* gene isolated from *Arachis hypogaea* to verify its genetic and functional diversity. Furthermore, expression pattern analysis of *AhFLS* and *AhLAR* in three selected cultivars of *A. hypogaea* has been determined to evaluate their genotype dependent expression. Comparative analysis was carried out to assess the association of flavonols and proanthocyanidins production with growth, biochemistry and antioxidant responses in *A. hypogaea* under the influence of salinity induced oxidative stress. Although FLS and LAR have been characterized in numerous plant species, but this study is the first ever detailed report on FLS and LAR in *A. hypogaea*. The findings of this study would assist in understanding the accumulation pattern of flavonols and proanthocyanidins under salinity stress and would aid in the development of a salt tolerant variety through metabolic engineering.

2. Materials and methods

2.1. Plant material and salt treatments

Seeds of three commercial cultivars of *A. hypogaea* (*A. hypogaea* cv. Bari 2011, *A. hypogaea* cv. BARD 92 and *A. hypogaea* cv. Golden) were collected from National Agriculture Research Centre (NARC), Islamabad, Pakistan based on the yield potential. Among them, Bari 2011 is a high yielding cultivar (yield potential = 6300 Kg/ha), Golden has a moderate yield potential of 4100 Kg/ha and BARD 92 has a yield potential of 2500 Kg/ha. (Naeem-ud-Din et al., 2012; Saeed and Hassan, 2009). Dehusked seeds were surface sterilized by a method 70% v/v ethanol for 2 to 3 min and kept at 4 °C for two days to break dormancy. Seeds were sown in an autoclaved mixture of soil and coconut husk (1:1 ratio) in small pots and kept in a glass house chamber at 28 °C under 16/8 h light/dark condition. Plants were watered according to field capacity measured through the difference in saturated wet and completely dried weight of potting media (Lopez and Barclay, 2017). Salt treatment was given to three groups of two-week-old seedlings. NaCl solution was added at concentrations of 0 mM, 60 mM, 120 mM, and 240 mM, respectively, for two weeks on alternate days according to the field capacity (Chavan and Karadge, 1980). The tissue samples were collected in plastic tubes on day 15 of the treatment and frozen immediately in liquid nitrogen followed by storage at −80 °C for evaluation of antioxidant enzymes activities, biochemical and expression analysis. Remaining plant parts were harvested for measuring the difference in growth and moisture content among the treatments.

2.2. Growth measurement and moisture content analysis

The length (cm), fresh and dry weight (g) of both shoot and root were recorded for control and treated plants after harvest. The fresh weight was measured instantly at the time of harvest. For evaluating dry weight, same plant samples were wrapped in aluminum foil and placed in a drying oven for three days at 70 °C. The dry and fresh weight of both root and shoot were used to determine the percentage of moisture content in control and treated groups by using the formula (dry weight - fresh weight) / fresh weight × 100 (Pokhrel and Dubey, 2013). All experiments were performed in triplicate.

2.3. Biochemical assays

The effect of salinity on chlorophyll, soluble sugar and soluble protein contents was evaluated through spectrophotometric methods from leaf samples. The ethanol method was used to determine leaf chlorophyll content (Lichtenthaler, 1987) and the optical density (OD) was measured at 666 nm using UV Visible Spectrophotometer (AE-S70-2U). The final estimation of chlorophyll content in mg/mg FW was calculated by the formula (OD of chlorophyll − 0.01) × 10 / (92.6474 × Dry weight of sample). The concentration of soluble sugar was evaluated by using a glucose standard curve after measuring OD of the sample at 490 nm following the methodology of Dubois (Dubois et al., 1956; Zhang and Huang, 2013). Total soluble protein was determined by recording OD at 595 nm using the Bradford assay (Bradford, 1976) after protein extraction (Elavarthi and Martin, 2010). The final concentration was evaluated through bovine serum albumin (BSA) standard curve analysis.

2.4. Enzymatic assays

The extracted proteins were further analyzed for the antioxidant activity of CAT, APX and SOD. CAT activity was estimated by measuring the decrease in the absorbance (Ab) at 240 nm by using diluted leaf extract according to Abei's protocol (Aebi, 1984). Final CAT activity was calculated by extinction coefficient (EC) of H_2O_2 (39.4 mM/cm at 240 nm) using the formula (change in Ab × total volume) / (sample volume × EC × min × Fresh weight). APX activity for each sample was recorded in mM/gFW by using EC (2.8 mM/cm), using the same formula as for CAT after taking OD of 3 mL mixture prepared by using the methodology of Nakano (Nakano and Asada, 1981) at 290 nm for 2 min with an interval of 30 s. However, SOD activity was measured by following the methods described by Beauchamp (Beauchamp and Fridovich, 1971). OD of both non-illuminated and illuminated sets of Ab was recorded at 560 nm and SOD activity was calculated through (Ab of sample - Ab of blank) / Ab of control (50/100).

2.5. RNA isolation and cDNA synthesis

Fresh leaves of *A. hypogaea* were subjected to total RNA extraction through TRIzol method (Jaakola et al., 2001). The pellet of RNA was dissolved in nuclease free water. The integrity and quality of RNA was evaluated through agarose gel electrophoresis, while it was quantified using Nanodrop spectrophotometer (Thermo Scientific, Wilmington, DE, USA). 1 μg of extracted RNA was used for cDNA synthesis using oligodT primer through RevertAid First Strand cDNA Synthesis Kit by Thermo Fisher Scientific.

2.6. Identification and isolation of AhFLS and AhLAR

The full-length coding sequences (CDS) of *AhFLS* (XM_025812267.1) and *AhLAR* (XM_025846016.1) was retrieved from National Center for Biotechnology Information (NCBI) and confirmed by genome sequences of *A. hypogaea* from PeanutBase (Bertioli et al., 2015). The nucleotide and amino acid sequences of *AhFLS* and *AhLAR* were analyzed through BLAST, respectively. Best hit published genes sequences were retrieved from GeneBank and aligned with *AhFLS* and *AhLAR*, respectively, through multiple sequence alignment tool of Geneious version 9.1.5 at default settings (Kearse et al., 2012). Reverse Transcription-polymerase chain reaction (RT-PCR) primers were designed from conversed region of both *AhFLS* and *AhLAR*, respectively (Table S1). Successfully amplified products were cleaned through ExoSAP-IT™ PCR Product Cleanup Reagent (Thermo Scientific, Wilmington, DE, USA) and transformed with pCR™2.1 Vector of TA Cloning™ Kit (Thermo Scientific, Wilmington, DE, USA) into the competent cells of E. coli DH5α through electroporation. Confirmed transformed clones were subjected to Sanger sequencing. Newly obtained sequences of *AhFLS* and *AhLAR* were submitted to NCBI for accession number and used for *in silico* analysis.

2.7. In silico analysis

Newly obtained *AhFLS* and *AhLAR* gene sequences were translated through ExPASy translate tool. Both nucleotide and amino acid sequence of *AhFLS* and *AhLAR* were analyzed by BLAST. Best hit published genes sequences were retrieved from GeneBank and aligned with *AhFLS* and *AhLAR* through multiple sequence alignment tool of Geneious version 9.1.5 (Kearse et al., 2012) at default setting. Phylogenetic analysis was performed through the Geneious tree builder tool using maximum likelihood method. Furthermore, *AhFLS* and *AhLAR* gene sequences were analyzed to determine the protein family using motif finder server (https://www.genome.jp/tools/motif/). While active site was predicted from online tool COFACTOR (https://zhanglab.ccmb.med.umich.edu/COFACTOR/). PeanutBase (Bertioli et al., 2015) were used to predict promoter region sequences approximately 1500 bp upstream to 5′ end of *AhFLS* and *AhLAR* gene and then analyzed for *cis*-regulatory elements using PlantCARE database (Lescot et al., 2002).

The conserved domains of *AhFLS* and *AhLAR* were identified through Conserved Domain Database (CDD), NCBI. The protein sequence of *AhFLS* and *AhLAR* were used to calculate molecular weight and theoretical isoelectric points through Compute pI/Mw tool of ExPASy protparam tool (https://web.expasy.org/protparam/) (Gasteiger et al., 2005). Furthermore, putative target localization of *AhFLS* and *AhLAR* was predicted by using WoLF PSORT (Horton et al., 2007). Secondary structure of *AhFLS* and *AhLAR* were predicted through PSI-blast based secondary structure prediction (PSIPRED) and Chou and fasman secondary structure prediction (CFSSP) server (http://www.biogem.org/tool/chou-fasman/). The three-dimensional (3D) protein structures were predicted through SWISS-MODEL ExPASY (Schwede et al., 2003) and demonstrated with the PyMOL viewer. The predicted protein model of *AhFLS* and *AhLAR* were evaluated and verified from ERRAT, QMEAN and Ramachandran plot. The model in the specified (.pdb) format was submitted to Protein Model Database (PMDB).

2.8. Expression analysis of AhFLS and AhLAR

Relative expression of *AhFLS* and *AhLAR* were determined in leaf samples of control and salt treated plants of three cultivars of *A. hypogaea* using real-time polymerase chain reaction (RT-qPCR). Maxima SYBR Green/ROX qPCR Master Mix by Thermo Fisher Scientific was used in Real-Time PCR in 7300 Fast Real-Time PCR system (Applied Biosystem, U.S.A.). Livak method ($2^{-\Delta\Delta Ct}$ method) was used for calculating fold change in expression and actin was used as a housekeeping gene (Livak and Schmittgen, 2001). Each sample was analyzed in triplicate. Primer sequences used in Real-Time PCR has been given in Table S1.

2.9. Fluorescence spectroscopy

Fluorescence spectra of both control and salt treated samples of the three cultivars of *A. hypogaea* on day 15 of the salt treatment were obtained using the spectrofluorometer system (FluoroMax-4, Horiba Scientific, USA) operated via FluorEssence software version 3.5, Horiba Scientific, USA. 150 W ozone free, xenon arc-lamp was a source of continuous wavelength light and an R928P photomultiplier tube with photon-counting detector as the signal detector (Ali et al., 2018). Synchronous spectra (Excitation range: 200–700 nm, offset: 60) for evaluating flavonoids in freshly plucked leaf samples from both control and treated groups were used for assessing spectral deviation. Three leaves from each of the replicates were used to analyze each study group. Flavonoids in root were detected at 380 nm as excitation wavelength and emission spectra range: 395–550 nm for all studied groups. Thoroughly washed tap roots were used for fluorescence spectroscopy immediately after their uprooting from the soil. The fluorescence spectrum for tap roots was recorded twice for each of the replicates. Spectra generated from leaves and roots were processed and analyzed through Origin software (OriginLab Corporation, USA) and GraphPad Prism® version 5.01 (GraphPad Software Inc., San Diego, CA, USA). Fluorescence spectra of both leaves and root for each variety were analyzed separately for spectral deviation between control and treated groups. Preprocessing of obtained fluorescence spectra involve removal of outliers and normalization while ANOVA was performed for inferential statistics of the obtained data.

2.10. Data analysis

Data collected from growth measurement, moisture content analysis, antioxidant enzyme activity, biochemical analysis and expression analysis were subjected to descriptive and inferential statistics. Microsoft® office 365 Excel and GraphPad Prism® version 5.01 (GraphPad Software Inc., San Diego, CA, USA) were used to organize and analyze data. Analysis of variance (ANOVA) followed by Bonferroni post hoc test was used to evaluates variance among control and treated groups. p-value smaller than 0.05 was considered as statistically significant in the given study. To check the dependability of expression of *AhFLS* and *AhLAR* with other variables, Pearson correlation test were performed using GraphPad Prism® version 5.

Table 1
Physiochemical properties of *Flavonol synthase* (FLS)from different plant species.

Gene	Protein accn.No.	Gene accn. No.	Aa	Mw	pI	II	AI	EC	GRAVY
A. hypogaea FLS	RYQ99263.1	XM_025812267.2	334	38.18	6.03	39.30	80.99	58,455	−0.543
A. duranensis FLS	XP_015931954.1	XM_016076468.2	334	38.31	5.82	41.97	81.29	58,455	−0.544
A. ipaensis FLS	XP_016167304.1	XM_016311818.2	334	38.18	6.03	39.30	80.99	58,455	−0.543
S. guianensis FLS	QHQ74395.1	MN165118.1	334	38.30	6.29	38.52	80.42	62,465	−0.539
G. max *FLS*	NP_001237419.1	NM_001250490.2	334	38.15	5.81	46.37	81.32	55,600	−0.513

Number of amino acids (aa), Molecular weight (Mw), Theoretical pI, Extinction coefficient (EC), Instability index (II), Aliphatic index (AI), Grand average of hydropathicity (GRAVY).

Table 2
Physiochemical properties of *Leucoanthocyanidin reductase* (*LAR*)from different plant species.

Gene	Protein accn.No.	Gene accn. No.	Aa	Mw	pI	II	AI	EC	GRAVY
A. hypogaea LAR		MH823866	351	38.72	5.94	34.26	89.72	21,930	−0.126
A. duranensis LAR	XP_015967593.1	XM_016112107.2	351	38.73	5.80	32.68	89.72	21,430	−0.119
A. ipaensis LAR	XP_016203013.1	XM_016347527.2	351	38.75	5.94	34.29	90.83	21,430	−0.113
L. uliginosus LAR	AAU45392.1	AY730617.1	348	38.34	7.07	27.40	92.47	26,400	−0.056
L. corniculatus LAR 1–2	ABC71325.1	DQ349101.1	349	38.56	8.08	31.25	90.50	26,400	−0.095
C. cajan LAR	XP_020233704.1		368	41.20	5.59	28.58	89.48	27,390	−0.213
G. max *LAR*	NP_001352050.1	NM_001365121.1	365	40.32	5.78	36.93	95.01	22,920	−0.049
V. angularis LAR	XP_017413424.1	XM_017557935.1	348	38.72	5.89	30.27	95.20	26,400	−0.054

Number of amino acids (aa), Molecular weight (Mw), Theoretical pI, Extinction coefficient (EC), Instability index (II), Aliphatic index (AI), Grand average of hydropathicity (GRAVY).

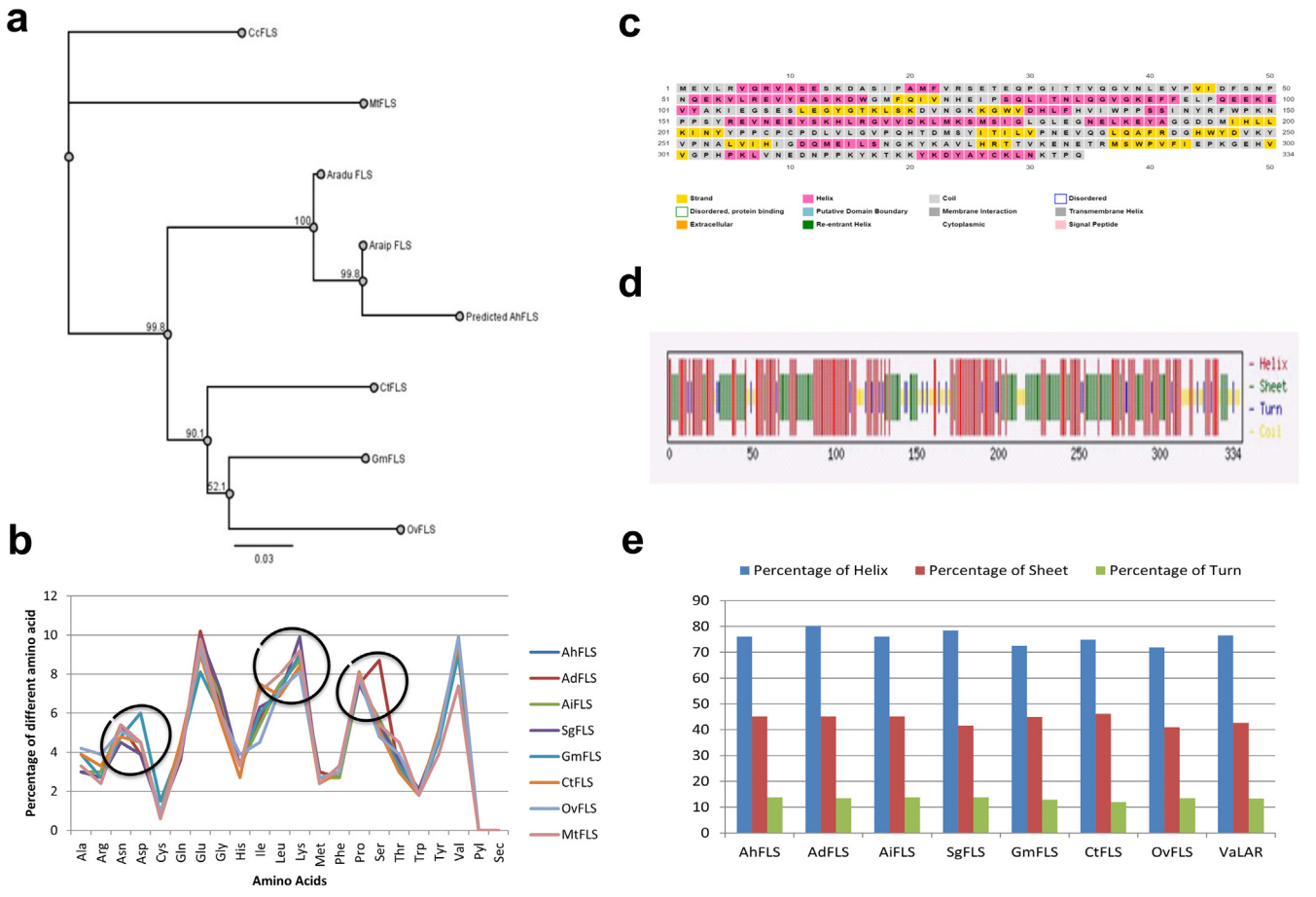

Fig. 1. Phylogenetic analysis of *AhFLS* and secondary structure analysis of putative protein sequence of *AhFLS* **a** Phylogenetic tree based on maximum likelihood **b** Amino acid composition analysis of *AhFLS* in comparison with FLS from other plant species **c, d** Secondary structure analysis of *AhFLS* **e** Percentage of helixes, sheets and turns of FLS in different plants.

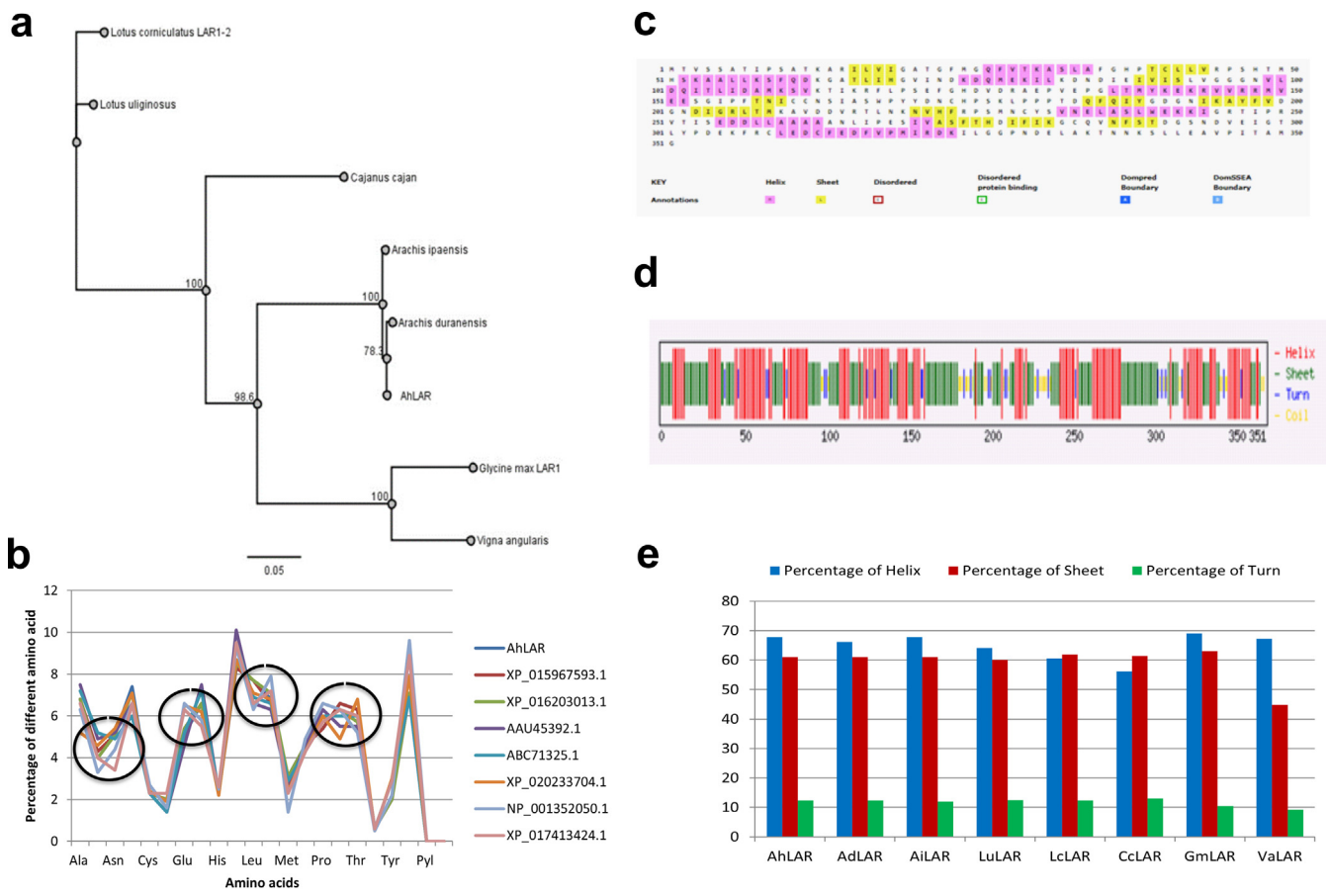

Fig. 2. Phylogenetic analysis of *AhLAR* and secondary structure analysis of putative protein sequence of *AhLAR* **a** Phylogenetic tree based on maximum likelihood **b** Amino acid composition analysis of *AhLAR* in comparison with LAR from other plant species **c, d** Secondary structure analysis of *AhLAR* **e** Percentage of helixes, sheets and turns of LAR in different plants.

3. Results

3.1. Sequence analysis of AhFLS and AhLAR

cDNA sequence of *Flavonol synthase* and *Leucoanthocyanidin reductase* from *A. hypogaea* designated as *AhFLS* (GenBank accession no. MT994314) and *AhLAR* (GenBank accession no. MH823866), respectively. The nucleotide sequence of *AhFLS* was 1343 bp that contained open reading frame (ORF) of 1004 bp encoding a predicted protein sequence of 334 amino acid. On the other hand, the nucleotide sequence of *AhLAR* was 1083 bp that contained ORF of 1056 bp encoding a predicted protein sequence of 351 amino acid. The calculated physiochemical parameters of predicted *AhFLS* and *AhLAR* protein in comparison to FLS and LAR protein from other plants have been listed in Table 1 and Table 2, respectively.

The analysis of amino acid composition indicated that predicted protein sequences of *AhFLS* contained high content of Val (9.6%), Glu (9%), Lys (8.7%), Leu (7.5%), Pro (7.5%), Gly (6.9%), Ser (5.7%) and Ile (5.4%), while predicted protein sequences of *AhLAR* contained high content of Ile (8.3%), Leu (7.7%), Asp (7.4%), Val (7.3%), Lys (6.8%), Ala (6.8%), Gly (6.6%), Ser (6.6%), and Thr (6.3%). The comparative amino acid composition analysis of LAR and FLS protein from various plants have been graphically presented in Fig. 1b and Fig. 2b. Secondary structure analysis revealed 76% α-helix, 45.2% sheets, 13.8% turns in predicted *AhFLS* protein and 67.8% α-helix, 61% sheets, 12.3% turns in predicted *AhLAR* as compared to FLS and LAR from other plant species, respectively (Fig. 1e and Fig. 2e).

AhFLS showed 100% similarity with the retrieved *AhFLS* (XM_025812267.2) sequence and *AhLAR* (MH823866.1) showed 100% similarity with the retrieved *AhLAR* (XM_025846016.1) sequence (Fig. S3 and Fig. S5). Protein-protein blast revealed that the predicted *AhLAR* protein sequence shared 72.63%, 73.35%, 73.07%, 73.64%, and 72.91% identity with *LAR* proteins from *Cajanus cajan (XP_020233704.1)*, *Glycine* max *LAR1(NP_001352050.1)*, *Lotus corniculatus LAR 1* (ABC71325.1), *Lotus uliginosus (AAU45392.1)* and *Vigna angularis* (XP_017413424.1), respectively. It also showed identity with its wild parents *Arachis ipaensis* (XP_016167304.1, 99.43%) and *Arachis duranensis* (XP_015931954.1, 99.43%). Whereas, predicted *AhFLS* protein sequence shared 91.32%, 83.53%, 83.93%, 82.62%, 82% and 79% identity with *FLS* proteins from *Stylosanthes guianensis* (*SgFLS*, QHQ74395.1), *Glycine* max (*GmFLS*, NP_001237419.1), *Clitoria ternatea* (*CtFLS*, BAF49296.1), *Onobrychis viciifolia* (*OvFLS*, AEF14416.1), *Medicago truncatula* (*MtFLS*, XP_003614780.1). It also showed identity with its wild parents *Arachis ipaensis* (XP_016167304.1, 100%) and *Arachis duranensis* (XP_015931954.1, 99.7%) (Fig. S4 and Fig. S6).

3.2. Phylogenetic analysis

Phylogenetic analysis of *AhFLS* resolved two distinct groups with the closest relationship to its wild parents: *A. ipaensis (Araip FLS)* and *A. duranensis (Aradu FLS)* (Fig. 1a). It also showed homology with *C. ternatea (CtFLS), G.* max *(GmFLS)* and *O. viciifolia (OvFLS).* This analysis also predicts that *AhFLS* evolved later in history. The analysis of the phylogenetic tree revealed that *AhLAR*

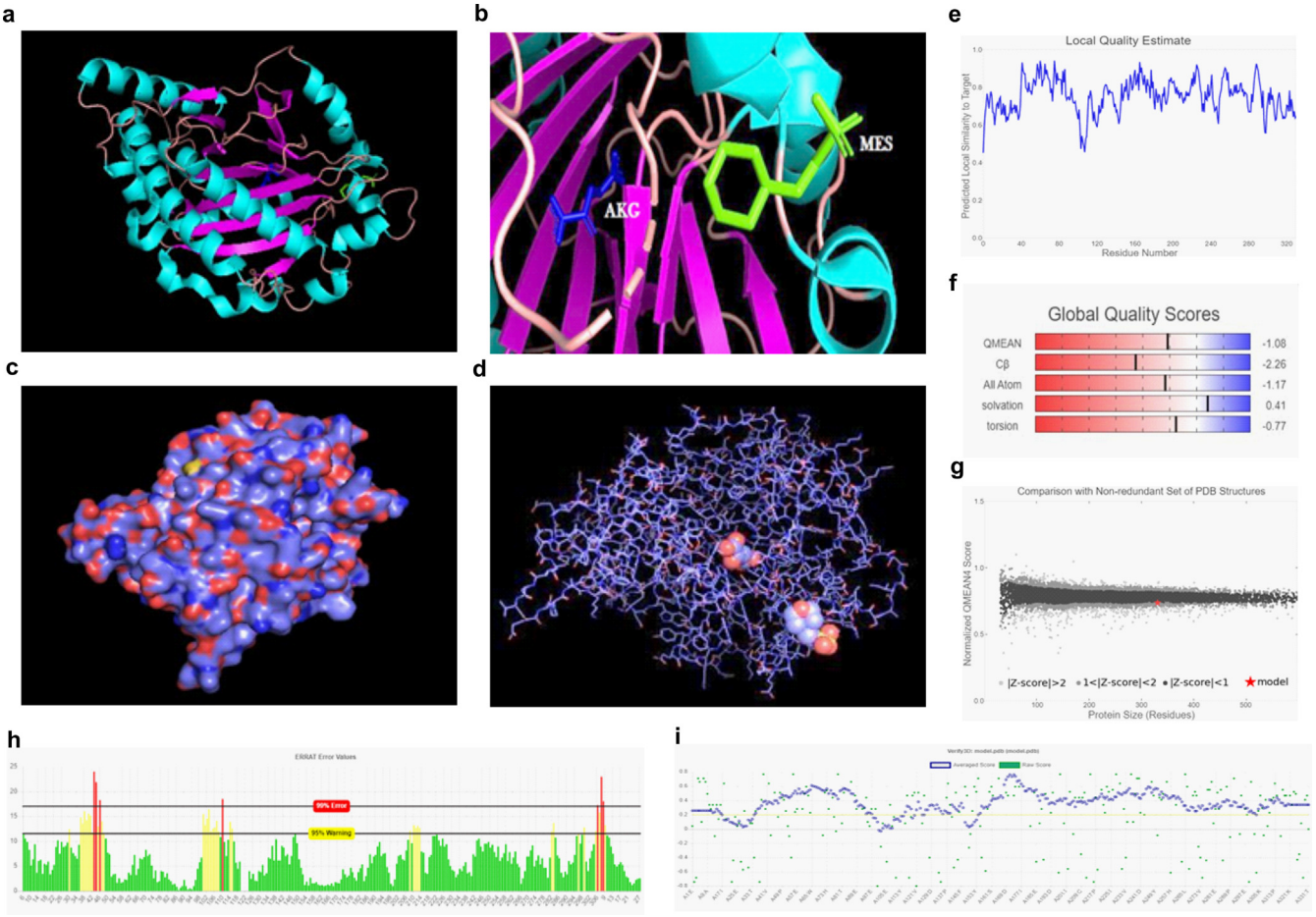

Fig. 3. Predictive three-dimensional structure of *AhFLS* and its assessment **a** Tertiary structure showing clear secondary arrangements and disulfides (Cyan Blue = Helix, Pink = Sheet, Grey = Loop) **b** Presumed catalytic sites with ligand AKG (2-Oxoglutaric Acid) and MES 2-(N-morpholino)ethanesulfonic acid) are indicated in blue and green respectively **c** Hydrophobic surface of the *AhFLS* **d** Detailed atomic structure of the *AhFLS*.

gene in *A. hypogaea* had an early origin in the evolutionary history as compared to similar genes in other plant species. The candidate gene is closely related to *A. duranensis, A. ipaensis, Stylosanthes guianensis*, *Glycine* max, *Clitoria ternatea*, *Onobrychis viciifolia* and *Medicago truncatula* (Fig. 2a).

3.3. 3D protein model of AhFLS and AhLAR

Three-dimensional model of *AhFLS* and *AhLAR* were predicted through homology modeling using SWISS-MODEL Expasy (Fig. 3 and Fig. 4). *AhLAR* depicted the highest model homology with *Leucoanthocyanidin reductase* from *Vitis vinifera*:3i52.1 (67.67%). The oligostate of the predicted protein model was a monomer with resolution of 2.28 Å. The predicted model of *AhLAR* (PMDB ID: PM0083389) has QMEAN4 and QMEAN6 scores are −0.53 and −0.74, respectively. SAVES server verified 3D score to be more than 80%. The 3D-model showed 92.50% of residues have an average 3D-1D score of $\geq$ 0.2. Therefore, the model is acceptable. At least 80% amino acid scored $\geq$ 0.2. This protein model showed the ERRAT value of 95.6332 for both chains. Analysis of Ramachandran plot showed that 95.8% residues resided in the favored region whereas 3.8% of residues were in allowed regions and the remaining 0.4% residues were present in generously allowed or outer region (Fig. S12).

Whereas *AhFLS* showed the highest model homology with *Flavonol synthase* from *Arabidopsis thaliana*:1gp4 (40.61%). The oligostate of the predicted protein model was a monomer with the resolution of the structure was 2.28 Å. The predicted model of *AhFLS* (PMDB ID: PM0083390) has QMEAN4 score of −1.08 and 3D score to be more than 80%. The 3D-model showed 87.31% of residues have an average 3D-1D score of $\geq$ 0.2. Therefore, the model is acceptable. At least 80% amino acid scored $\geq$ 0.2. This protein model showed the ERRAT value of 87.1473 for both chains. Analysis of Ramachandran plot showed that 93.4% residues resided in the favored region whereas 5% of residues were in allowed regions and the remaining 0.6% residues were present in generously allowed or outer region (Fig. S11).

3.4. Functional analysis of AhFLS and AhLAR

A similar pattern was observed in both protein and nucleotide sequences after multiple sequence alignment. CDD search revealed that the deduced *AhFLS* protein has putative conserved domains belonging to the 2OG-Fe(II) oxygenase superfamily domain (pfam03171, 200–295), a highly conserved N-terminal region of proteins with *2-oxoglutarate/Fe(II.)-dependent dioxygenase* activity and the *AhFLS* domain (PLN02704, 2-191) (Fig. S1). However, NADB_Rossmann Superfamily domain has been identified for *AhLAR* (Fig. S2).

The active site amino acid residues of *AhLAR* were predicted to be Cys and Asp while as that of *AhFLS* were Leu, Lys, Cys, Glu, Gln, Ile and His as determined by COFACTOR. Due to the unavailability of any direct method for identifying the active site amino acids of *AhLAR* and *AhFLS*, the sequence information of closest homology

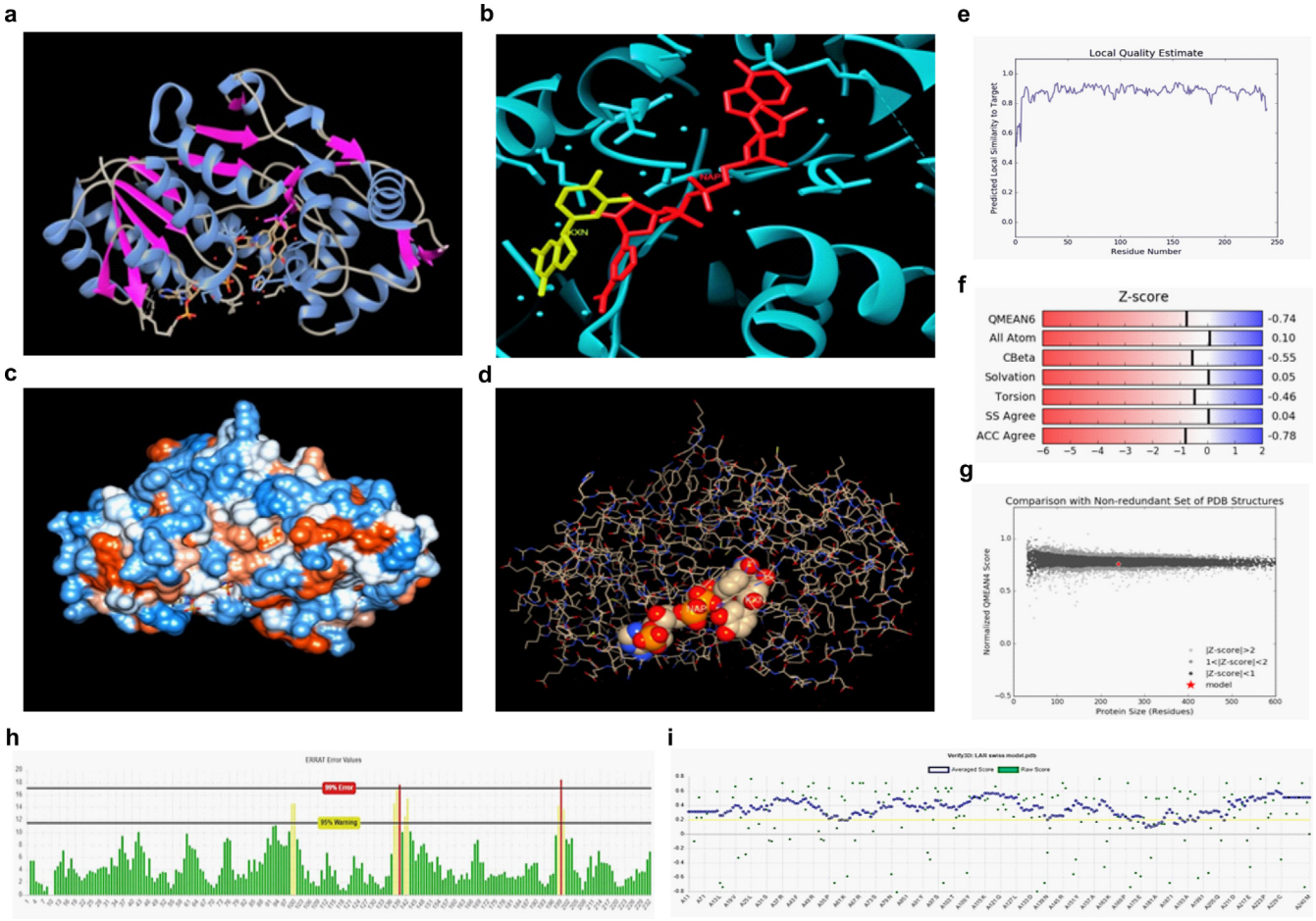

Fig. 4. Predictive three-dimensional structure of *AhLAR* and its assessment **a** Tertiary structure showing clear secondary arrangements and disulfides (Cyan Blue = Helix, Pink = Sheet, Grey = Loop) **b** Presumed catalytic sites with ligand NAP (nicotinamide-adenine-dinucleotide phosphate) and KXN (2R,3S)-2-(3,4-Dihydroxyphenyl)-3,4-dihydro-2H-chromene-3,5,7-triol; tetrahydrate are indicated in red and yellow, respectively **C** Hydrophobic surface of the *AhLAR* **d** Detailed atomic structure of the *AhLAR*.

Table 3
Putative *Cis* regulatory elements in the promoter region of *AhFLS*.

Class	*Cis* Regulatory Element Name	Position	Core Sequence	Putative Function
Environmental stress responsive	5UTR Py-rich stretch			Involved in Biotic Stress
	ARE	496,1461	AAACCA, AAACCA	Involved in anaerobic induction
Hormone signalling	TCA-element	1195	CCATCTTTTT	Involved in the salicylic acid responsiveness
	TGACG-motif	1092	TGACG	Involved in the MeJA-responsiveness

Table 4
Putative *Cis* regulatory elements in the promoter region of *AhLAR*.

Class	*Cis* Regulatory Element Name	Position	Core Sequence	Putative Function
Development responsive	RY-element	604	CATGCATG	*Cis* acting regulatory element involved in seed-specific regulation
Light Responsive	G box	628	CACGTC	Light responsiveness
	AE-box	1391	AGAAACAA	Light responsiveness
	Box 4	254, 267	ATTAAT, ATTAAT	Light responsiveness
Hormone signalling	CGTCA-motif	630	CGTCA	MeJA-responsiveness
	TATC-box	531	TATCCCA	Gibberellin-responsiveness
MYB binding site	CCAAT-box	1396	CAACGG	MYBHv1 binding site

putative *leucoanthocyanidin reductase 1* from *Vitis vinifera* (PDB ID: 3I52.1) and *Anthocyanidin synthase* from *Arabidopsis thaliana* (PDB ID: 1gp4.1) were used for identifying active site amino acid, respectively. Then, sequence alignment analysis was performed for aligning *AhLAR* with 2gasA and *AhFLS* with 1gp6A. Six functional motifs were detected from the functional study in case of *AhLAR*, which were found to be a member of NmrA-like family, NAD-dependent dehydratase family and 3, *β hydroxysteroid dehydrogenase* family (Fig. S8). On the other hand, two functional motifs 2OG-FeII_Oxy and DIOX_N were detected from the functional study in case of *AhFLS*, which were found to be a member of 2OG-Fe(II) oxygenase superfamily (Fig. S7).

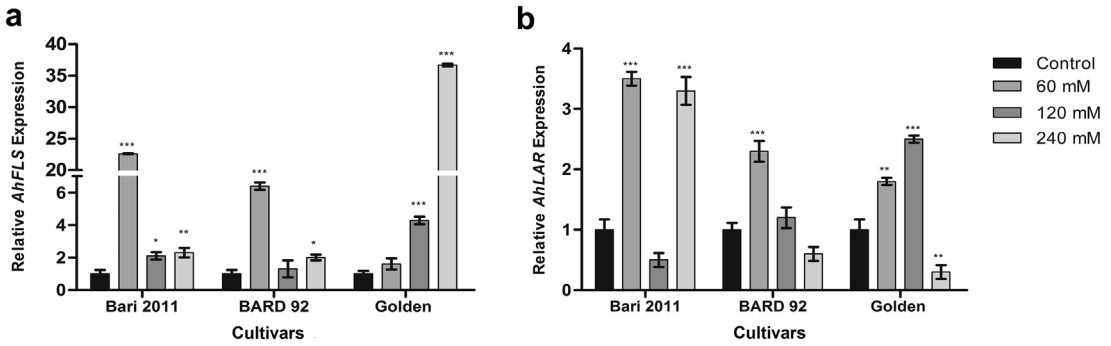

Fig. 5. Expression analysis of **a** *AhFLS* (Two-way ANOVA: Interaction *p*-value = < 0.0001, Column factor *p*-value = < 0.0001, Row factor *p*-value = < 0.0001) and **b** *AhLAR* (Two-way ANOVA: Interaction *p*-value = < 0.0001, Column factor *p*-value = < 0.0001, Row factor *p*-value = < 0.0001) in three selected varieties of *A. hypogaea* against salinity stress. Here, control represents internal comparison of individual cultivar.

3.5. Promoter sequence analysis

Cis-acting regulatory elements predicted using plantCARE database showed that both gene promoters contained typical eukaryotic regulatory elements including CAAT and TATA, Table 3 and Table 4. Furthermore, several other stress related promoter elements were identified in the promoter sequences of *AhFLS* and *AhLAR* which were classified into four groups based on the cellular mechanisms that modulate the development regulation, environmental stress responses, light-mediated responses and hormonal signaling. *MYB* binding site and hormonal responsive *cis*-regulatory element were also observed in the promoter regions of *AhFLS* and *AhLAR*.

3.6. Relative AhFLS and AhLAR expression in response to salinity

Expression of *AhFLS* and *AhLAR* against salinity stress has been evaluated to confirm their role in abiotic stress in peanut. Three distinct cultivars of *A. hypogaea* (Bari 2011, BARD 92 and Golden) were selected for analysis at various level of stress. Both *AhFLS* and *AhLAR* depicted differential expression against various concentration of salinity stress and confirmed their role in response to salinity (Fig. 5). Highest upregulation of *AhFLS* (36.7 fold increase) has been observed in Golden at highest concentration of salt (240 mM) while highest upregulation of *AhLAR* (3.5 fold increase) has been observed in Bari 2011 at 60 mM and 240 mM concentration of salt. *AhLAR* has been found to be positively regulated at lower concentrations of salt while negatively regulated at higher concentration of salt. However, *AhFLS* expression was quite contrary in different variety. In Golden, the gradual increase of *AhFLS* expression has been observed with the increase in salt concentration. However, Bari 2011 and BARD 92 showed highest upregulation of *AhFLS* at 60 mM.

3.7. Accumulation of flavonol and proanthocyanins in leaves

Leaf synchronous fluorescence spectra showed eight prominent fluorescent regions; low intensity bands at 330–350 nm, 378 nm, 579–605 nm, high intensity regions 390–425 nm, 681 nm, 725 nm and strong fluorescent regions between 449 and 466 nm, 510–552 nm with a sharp peak at 526 nm (Fig. 6). Fluorescent region between 330 and 350 nm has already been reported with the presence of catechins (Holser, 2014; Pal et al., 2012), approximately 350 nm emission maxima for proanthocyanidin, fluorescence emission with maxima at 378 nm with apigenin (Park et al., 2013; Tu et al., 2016), regions with fluorescence emission in the range of 390–425 nm and 449–466 nm represent both non-acylated flavonol glucosides that are present in plant cuticle (Donaldson and Williams, 2018); 510–552 nm for flavonol, flavones (Guharay et al., 2001; Voicescu et al., 2014) 395 nm for Reversetrol (Figueiras et al., 2011), 522 nm for curcumin, 440 nm polyphenolics (Singh and Mishra, 2015) and 334 nm tocopherol (Demirkaya-Miloglu et al., 2013) and 579–605 nm for anthocyanin (Drabent et al., 1999). Chlorophyll *b* and a emitted fluorescence at 681 nm and 725 nm (Weber and Teale, 1957). The fluorescent region between 360 and 560 nm has been studied due to their association with flavonol peaks including kaempferol ($\lambda_{em} \approx$ 463 nm), quercetin ($\lambda_{em} \approx$ 535 nm), rutin ($\lambda_{em} \approx$ 545 nm), morin ($\lambda_{em} \approx$ 490 nm) and non-acylated flavonol glucosides (Condat et al., 2016; Donaldson and Williams, 2018; Höfener et al., 2013; Tu et al., 2016; Xu et al., 2010). Higher fluorescence intensity was observed from 440 to 560 nm in salt treated groups as compared to the control in all three cultivars, which showed accumulation of flavonol during salt stress. The appearance of a fluorescence peak at 345 nm that represents catechins and tocopherol was only observed in Golden salt stressed plants at all salt concentrations whereas, that peak was only observed in Bari 2011 at 240 mM salt concentration.

3.8. Accumulation of flavonol and proanthocyanins in roots

The excitation of tap root at 380 nm yielded emission fluorescence spectra at a low intensity region (408–418 nm), two high intensity regions (435–443 nm and 450–480 nm) and a moderate intensity region (505–522 nm) (Fig. 7). Generally, all these fluorescent regions have been reported as emission spectra related to flavonol, chalcones, flavones and isoflavnoids (Asiri et al., 2014; de Rijke et al., 2002; Guharay et al., 2001; Voicescu et al., 2014). In Bari 2011, significant spectral variation has been observed in the region of 418 to 443 nm region that generally represents polyphenolics ($\lambda_{em} \approx$ 440 nm) (Singh and Mishra, 2015), 390–425 nm non-acylated flavonol glucosides (Donaldson and Williams, 2018). In BARD 92, spectra representing polyphenolics, non-acylated flavonol glucosides, *trans*-resveratrol ($\lambda_{em} \approx$ 395 nm) (Figueiras et al., 2011) (Fig. 6e). In Golden, region representing *trans*-resveratrol appeared in the control and 120 mM treated plants while significant spectral variation recorded in between 510 and 545 nm region that represents flavonols ($\lambda_{em} \approx$ 535 nm) and curcumin ($\lambda_{em} \approx$ 522 nm). Generally, all the three cultivars showed statistically significant spectral deviation as compared to their respective controls.

3.9. Correlation of AhFLS and AhLAR expression with biochemical and growth parameters

All three peanut cultivars were grown under salinity stress (0 mM, 60 mM, 120 mM, and 240 mM) resulting in different seedling lengths, fresh weight and moisture content as compared to their respective control plants after 15 days of salt treatment

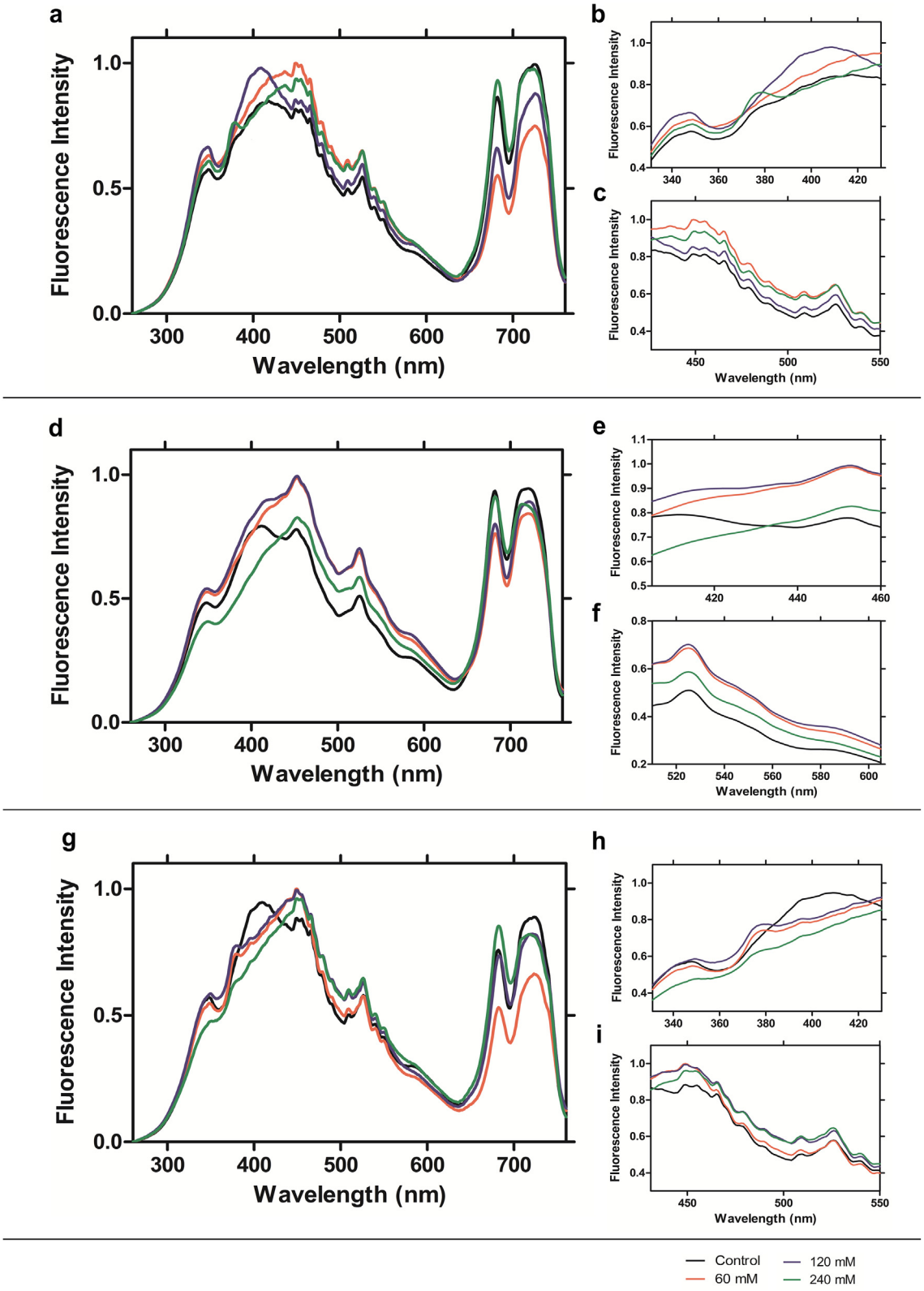

Fig. 6. Synchronous fluorescence spectra of leaves of three cultivar of peanut (Bari 2011, BARD 92 and Golden) showing spectral deviation at different salt concentrations with excitation range: 200–700 nm, offset: 60 **a** Fluorescence spectra of Bari 2011 leaves **b** Spectral deviation in Bari 2011 leaves in the region of 330 to 430 nm **c** Spectral deviation in the leaves of Bari 2011 in region of 435 to 550 nm **d** Fluorescence spectra of BARD 92 leaves **e** Spectral deviation in the leaves of BARD 92 in region of 400 to 460 nm **f** Spectral deviation in the leaves of BARD 92 in region of 510 to 610 nm **g** Fluorescence spectra of Golden leaves **h** Spectral deviation in the leaves of Golden in region of 330 to 430 nm **i** Spectral deviation in the leaves of Golden in region of 430 to 550 nm.

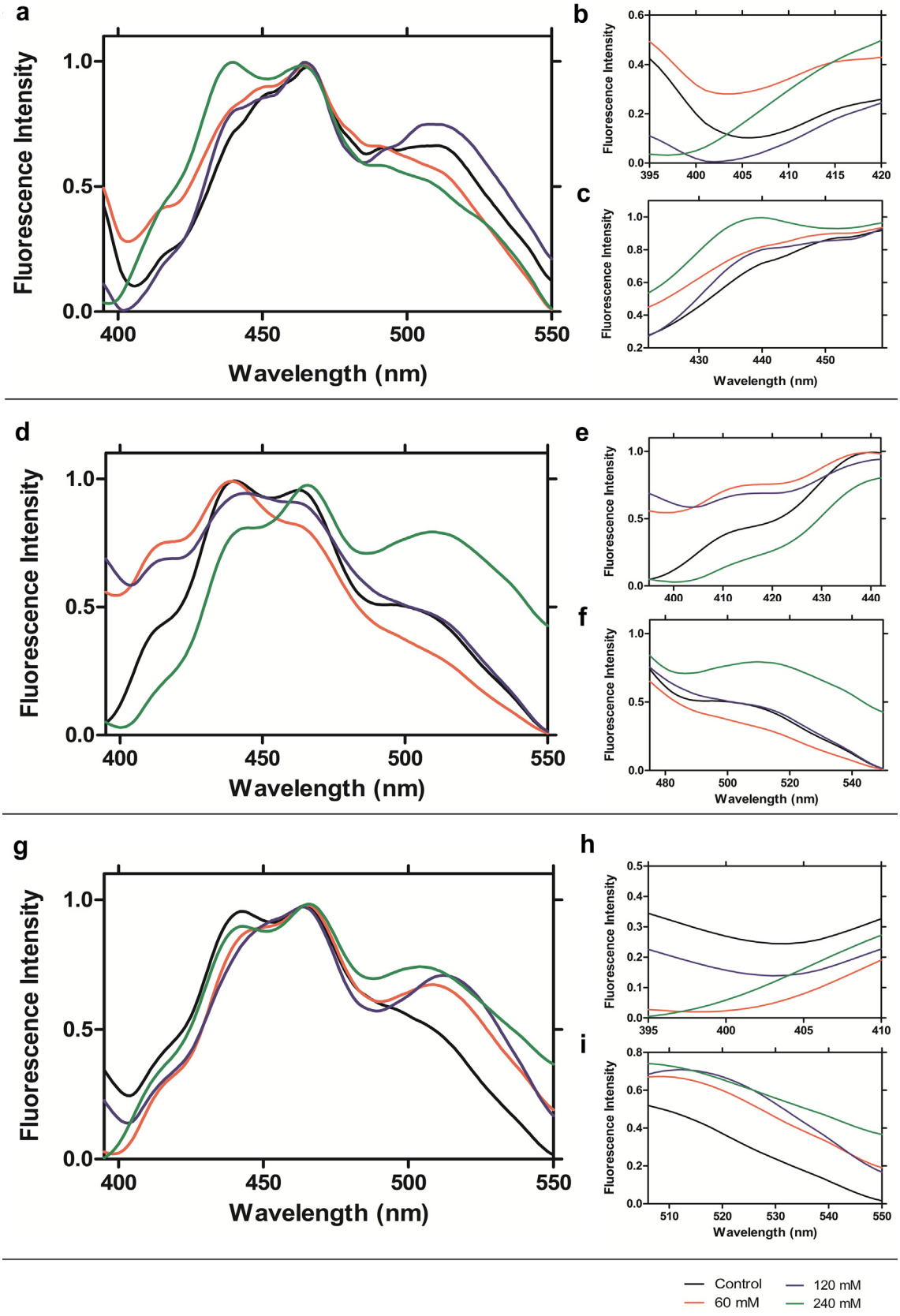

Fig. 7. Fluorescence spectra of tap root of three cultivar of peanut (Bari 2011, BARD 92 and Golden) showing spectral deviation at different salt concentrations after excitation at 380 nm (emission spectra range: 395–550 nm) **a** Fluorescence spectra of Bari 2011 tap roots **b** Spectral deviation in the tap roots of Bari 2011 in region of 395 to 420 nm **c** Spectral deviation in the tap roots of Bari 2011 in region of 425 to 450 nm **d** Fluorescence spectra of BARD 92 tap roots **e** Spectral deviation in the tap roots of BARD 92 in region of 490 to 440 nm **f** Spectral deviation in the tap roots of BARD 92 in region of 475 to 550 nm **g** Fluorescence spectra of Golden roots **h** Spectral deviation in the tap roots of Golden in region of 395 to 410 nm **i** Spectral deviation in the tap roots of Golden in region of 490 to 550 nm.

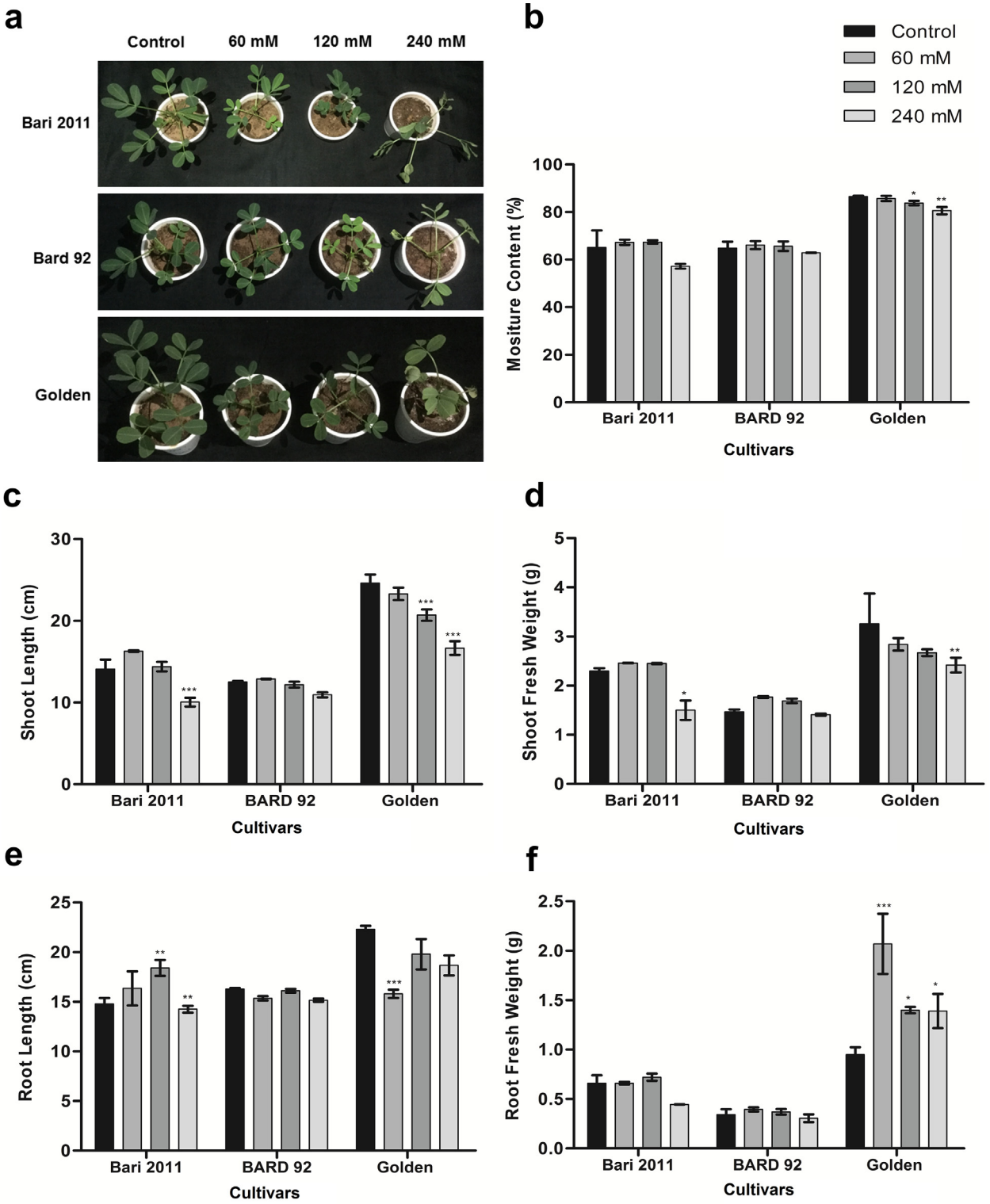

Fig. 8. Effects of salinity on growth and moisture content of three Pakistani cultivars of peanut (Bari 2011, BARD 92 and Golden) **a** Symptoms of salinity (wilting and browning) and gradual decease in overall growth of all three cultivars **b** Gradual decrease in moisture content with respect to increasing salt concentration (Two-way ANOVA: Interaction *p*-value = 0.6696, Column factor *p*-value = 0.0107, Row factor *p*-value = < 0.0001) **c** Relative shoot length of peanut cultivars under salinity (Two-way ANOVA: Interaction *p*-value = < 0.0001, Column factor *p*-value = < 0.0001, Row factor *p*-value = < 0.0001) **d** Shoot fresh weight under salinity (Two-way ANOVA: Interaction *p*-value = 0.1196, Column factor *p*-value = 0.0010, Row factor *p*-value = < 0.0001) **e** Relative root length of peanut cultivars under salinity (Two-way ANOVA: Interaction *p*-value = < 0.0001, Column factor *p*-value = 0.0006, Row factor *p*-value = < 0.0001) **f** Shoot fresh weight under salinity (Two-way ANOVA: Interaction *p*-value = < 0.0001, Column factor *p*-value = 0.0001, Row factor *p*-value = < 0.0001) . Data presented as mean ± S.E. *p*-value smaller than 0.05 is considered significant. '*' is depicting *p*-value<0.05, '**' *p*-value<0.01, '***' *p*-value<0.001.

(Fig. 8). Negative relationship has been observed in the expression of *AhFLS* and *AhLAR* with the root length. On contrary, positive relationship has been observed in the expression of *AhFLS* and *AhLAR* with the shoot length except *AhFLS* in Golden showed negative correlation with shoot length (r = -0.9209). Positive relationship has been observed in the expression of *AhFLS* and

Table 5
Correlation of *AhFLS* and *AhLAR* expression with antioxidant enzymes activity, biochemical and growth parameters.

Cultivars	FLS *vs.* RL		FLS *vs.* SL		FLS *vs.* RFW		FLS *vs.* SFW		FLS *vs.* MC		FLS *vs.* SC	
	r	*p*-value	*r*	*p*-value	*r*	*p*-value	*r*	*p*-value	*r*	*p*-value	*r*	*p*-value
Bari 2011	0.1582	0.8418	0.6316	0.3684	0.1897	0.8103	0.3862	0.6138	0.3997	0.6003	−0.4181	0.5819
BARD 92	−0.5957	0.4043	0.4651	0.5349	0.6258	0.3742	0.6570	0.3430	0.4574	0.5426	0.4713	0.5287
Golden	−0.1197	0.8803	−0.9209	0.0791	−0.08499	0.9150	−0.7582	0.2418	−0.9345	0.0655	0.8276	0.1724
	FLS *vs.* SP		**FLS *vs.* APX**		**FLS *vs.* CAT**		**FLS *vs.* SOD**		**FLS *vs.* Chlorophyll**		**FLS *vs.* LAR**	
	r	*p*-value	*r*	*p*-value	*r*	*p*-value	*r*	*p*-value	*r*	*p*-value	*r*	*p*-value
Bari 2011	−0.1324	0.8676	−0.3660	0.6340	0.6219	0.3781	−0.1154	0.8846	−0.3840	0.6160	0.6344	0.3656
BARD 92	0.1588	0.8412	−0.2759	0.7241	0.6422	0.3578	0.2347	0.7653	0.05184	0.9482	0.8802	0.1198
Golden	−0.4449	0.5551	0.8211	0.1789	0.9000	0.1000	−0.3991	0.6009	−0.8769	0.1231	−0.7155	0.2845
	LAR *vs.* RL		**LAR *vs.* SL**		**LAR *vs.* RFW**		**LAR *vs.* SFW**		**LAR *vs.* MC**		**LAR *vs.* SC**	
	r	*p*-value	*r*	*p*-value	*r*	*p*-value	*r*	*p*-value	*r*	*p*-value	*r*	*p*-value
Bari 2011	−0.4761	0.5239	−0.1886	0.8114	−0.6386	0.3614	−0.4658	0.5342	−0.4549	0.5451	0.3763	0.6237
BARD 92	−0.1563	0.8437	0.8056	0.1944	0.9145	0.0855	0.8814	0.1186	0.8239	0.1761	0.3316	0.6684
Golden	−0.1756	0.8244	0.3903	0.6097	0.3465	0.6535	0.1056	0.8944	0.4254	0.5746	−0.2220	0.7780
	LAR *vs.* SP		**LAR *vs* APX**		**LAR *vs.* CAT**		**LAR *vs.* SOD**		**LAR *vs.* Chlorophyll**			
	r	*p*-value	*r*	*p*-value	*r*	*p*-value	*r*	*p*-value	*r*	*p*-value		
Bari 2011	−0.3983	0.6017	0.1053	0.8947	0.4556	0.5444	−0.3351	0.6649	−0.4637	0.5363		
BARD 92	0.4899	0.5101	−0.6278	0.3722	0.5709	0.4291	0.2219	0.7781	0.2273	0.7727		
Golden	0.7767	0.2233	−0.1891	0.8109	−0.3790	0.6210	0.6965	0.3035	0.2920	0.7080		

FLS = Flavonol synthase; LAR = Leucoanthocyanidin reductase; RL = Root Length; SL = Shoot Length; RFW = Root Fresh Weight; SFW = Shoot Fresh Weight; MC = Moisture Content; SC = Sugar Contents; SP = Soluble Protein; APX = Ascorbate peroxidase; CAT = Catalase; SOD = Superoxide dismutase.
r = Pearson *r* that is showing correlation between two variables.
p-value less than 0.05 is considered to be statistically significant.

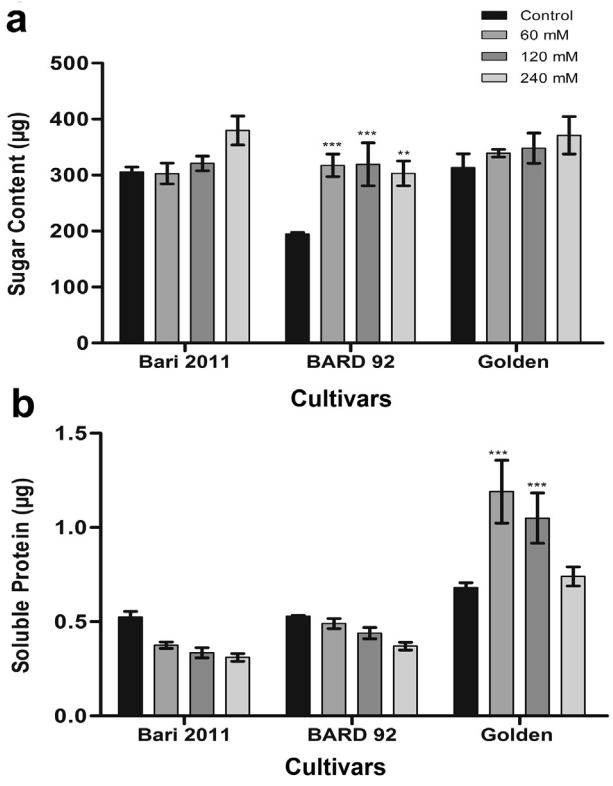

Fig. 9. Salinity affecting accumulation of soluble protein and sugar in three cultivars of peanut (Bari 2011, BARD 92 and Golden) **a** Enhanced accumulation of soluble sugar in all the three verities of peanut (Two-way ANOVA: Interaction *p*-value = 0.0805, Column factor *p*-value = 0.0004, Row factor *p*-value = 0.0010) **b** Salinity induced accumulation of soluble protein in Golden (Two-way ANOVA: Interaction *p*-value = < 0.0001, Column factor *p*-value = 0.0022, Row factor *p*-value = < 0.0001). Data presented as mean ± S.E. *p*-value smaller than 0.05 is considered significant. '**' is depicting *p*-value<0.01, '***' *p*-value<0.001.

AhLAR with root fresh weight, shoot fresh weight and moisture content in BARD 92. However, Golden and BARD 92 showed negative relationship in the expression of *AhFLS* and *AhLAR* with root fresh weight, shoot fresh weight and moisture content, respectively (Table 5).

In response to salinity stress, significant differential accumulation of soluble protein, sugar and chlorophyll has been observed within selected peanut cultivars (Fig. 9 and Fig. 10). Correlation studies has been conducted to evaluate the dependability of *AhFLS* and *AhLAR* expression on soluble protein, sugar, and chlorophyll content in plant cells. High level of negative correlation has been observed between chlorophyll content and *AhFLS* expression in Golden ($r = -0.8769$) while BARD 92 showed no relationship between *AhFLS* and chlorophyll content. Fair degree of negative correlation has been observed between chlorophyll content and *AhLAR* expression in Bari 2011 ($r = -0.4637$). The expression of *AhFLS* was found to dependable on soluble sugar than soluble protein while the expression of *AhLAR* was observed to dependable on soluble protein than soluble sugar (Table 5).

3.10. Correlation of AhFLS and AhLAR expression with antioxidant enzymes activity

Expression of APX, SOD, CAT, *AhFLS* and *AhLAR* have been observed to be influenced by salinity stress (Fig. 5 and Fig. 11). To observe association of *AhFLS* and *AhLAR* expression with the activity of antioxidant enzymes, Pearson's correlation was performed and revealed *AhFLS* has little or no relationship with SOD activity in Bari 2011 and BARD 92 (r = -0.1154 and r = 0.2347), fair relationship with SOD activity in Bari 2011 ($r = -0.3991$) and APX activity in Bari 2011 and BARD 92 ($r = -0.3660$ and $r = -0.2759$). Moderate relationship of *AhFLS* has been observed with CAT activity in Bari 2011 and BARD 92 ($r = 0.6219$ and $r = 0.6422$) while strong relationship of *AhFLS* has been observed with APX and CAT activity in Golden ($r = 0.8211$ and $r = 0.9000$). Moderate association of *AhLAR* has been observed with APX activity ($r = -0.6278$), CAT activity ($r = 0.5709$) in BARD

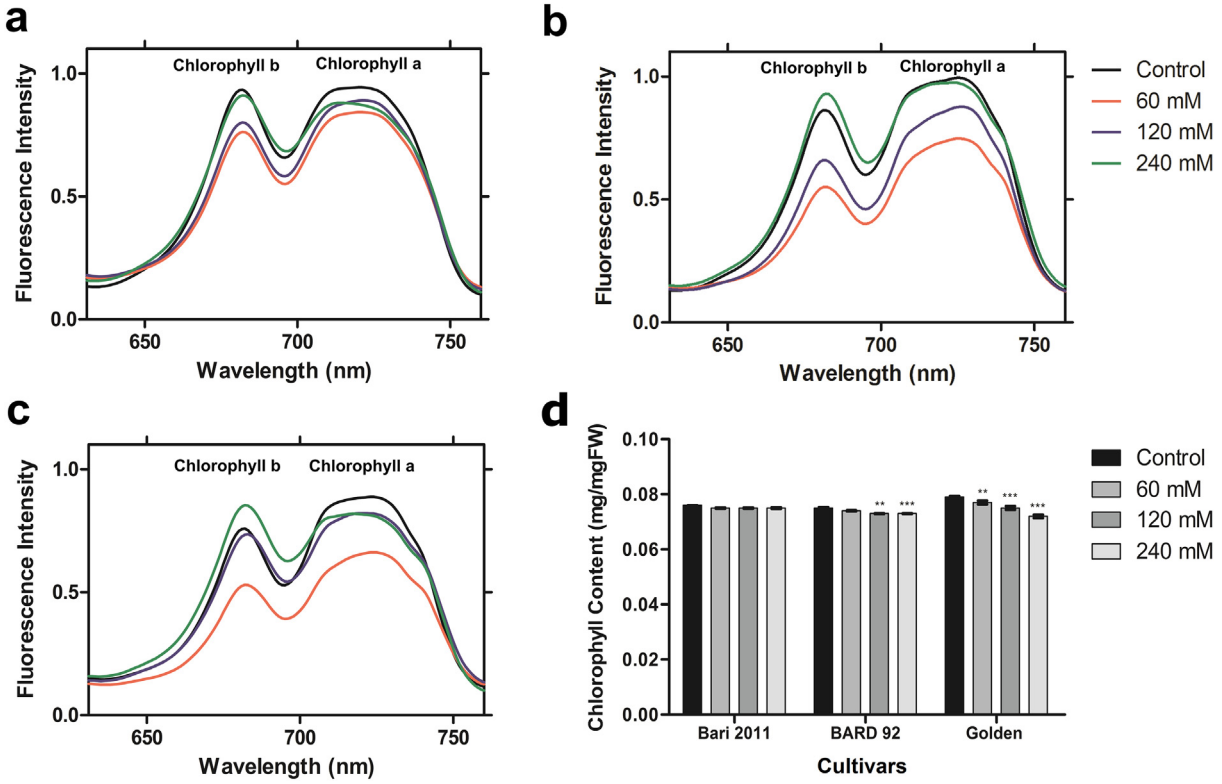

Fig. 10. Synchronous fluorescence spectra and chlorophyll analysis in three cultivars of peanut (Bari 2011, BARD 92 and Golden) **a** Fluorescence spectrum of Bari 2011**b** Fluorescence spectrum of BARD 92**c** Fluorescence spectrum of Golden **d** Effect of salinity on chlorophyll content of peanut seedlings through biochemical analysis (Two-way ANOVA: Interaction *p*-value = < 0.0001, Column factor *p*-value = 0.0022, Row factor *p*-value = < 0.0001). Each spectral line represents mean of replicates. Data of chlorophyll content presented as mean ± S.E. *p*-value smaller than 0.05 is considered significant. '**' is depicting *p*-value<0.01, '****' *p*-value<0.001.

92 and SOD activity in Golden (r = 0.6965). While fair or little association of *AhLAR* has been with APX and CAT activity in Bari 2011 and Golden (Table 5).

4. Discussion

FLS and LAR belong to two distinct branches of flavonoid biosynthetic pathway and lead to the production of flavonols and proanthocyanidins, respectively (Nabavi et al., 2018; Zhang et al., 2020). In the present study, FLS and LAR isolated from *Arachis hypogaea* have been structurally, transcriptionally, and functionally characterized. Furthermore, the oxidative stress generated by salinity has been used to evaluate the protective role *AhFLS* and *AhLAR* against stress in three selected cultivars of *A. hypogaea* (Bari 2011, BARD92 and Golden). cDNA sequence of *AhFLS* (MT994314) and *AhLAR* (MH823866.1) showed conservation of enzymes' sequence and functionality within varieties of *A. hypogaea* as 100% similarity has been observed in these enzymes with already published *AhFLS* (XM_025812267.2) and *AhLAR* (XM_025846016.1) sequence, respectively. The role conservation of *AhFLS* and *AhLAR* has been further analyzed within species through multiple sequence alignment and phylogenetic analysis which revealed that both genes are closely related to *A. duranensis, A. ipaensis, Stylosanthes guianensis*, *Glycine* max, *Clitoria ternatea*, *Onobrychis viciifolia* and *Medicago truncatula.* Phylogenetic study also showed that *AhFLS* evolved later in history while *AhLAR* had an early origin in peanut.

AhFLS and *AhLAR* showed highest model homology with *Flavonol synthase* from *Arabidopsis thaliana*:1gp4 and *Leucoanthocyanidin reductase* from *Vitis vinifera*:3i52.1. Based on sequence and structural similarities, functional analysis of *AhFLS* and *AhLAR* revealed that *AhFLS* has two functional motifs 2OG-FeII_Oxy and DIOX_N. The presence of these two functional domains indicated that *AhFLS* has part in the biosynthesis of flavonols in peanut plant (Hou et al., 2020). Whereas, *AhLAR* has six functional motifs that are related to NmrA-like family, NAD-dependent dehydratase family and 3, β *hydroxysteroid dehydrogenase* family that are crucial for the catalytic activity of LAR and consequent production of proanthocyanidins (Maugé et al., 2010). Cys and Asp are predicted as active site amino acid residues of *AhLAR* and Leu, Lys, Cys, Glu, Gln, Ile and His as that of *AhFLS.* Presence of stress related promoter elements in the promoter sequences of *AhFLS* and *AhLAR* their role in the regulation growth, development and stress responses.

Flavonols and proanthocyanidins have imperative role in the defense response against both biotic and abiotic stress in plants due to their free radical scavenging and antioxidant activity (Andersen and Markham, 2005;Muhlemann et al., 2018). The expression analysis of *AhFLS* and *AhLAR* along with the accumulation pattern of flavonols and proanthocyanidins in *A. hypogaea* indicated their role against salinity stress. Moreover, their expression and accumulation patterns were found to be genotype and stress-level dependent. Hence, indicating that their regulation is multivariate dependent. Higher differential accumulation in the roots rather than in the leaves of *A. hypogaea* confirmed that they specifically accumulate in the roots of *A. hypogaea.* Many flavonoids are found to be accumulated specifically in the root regions such as nodule primordia and lateral roots of the clover (Trifolium subterraneum) (Djordjevic et al., 1997; Morris and Djordjevic, 2006) and in root primordia and root tip of A. thaliana (Buer et al., 2007; Peer et al., 2001).

Correlation of AhFLS and AhLAR expression with antioxidant enzymes activity, biochemical and growth parameters revealed negative, positive or no relation, but no statistically significant p-

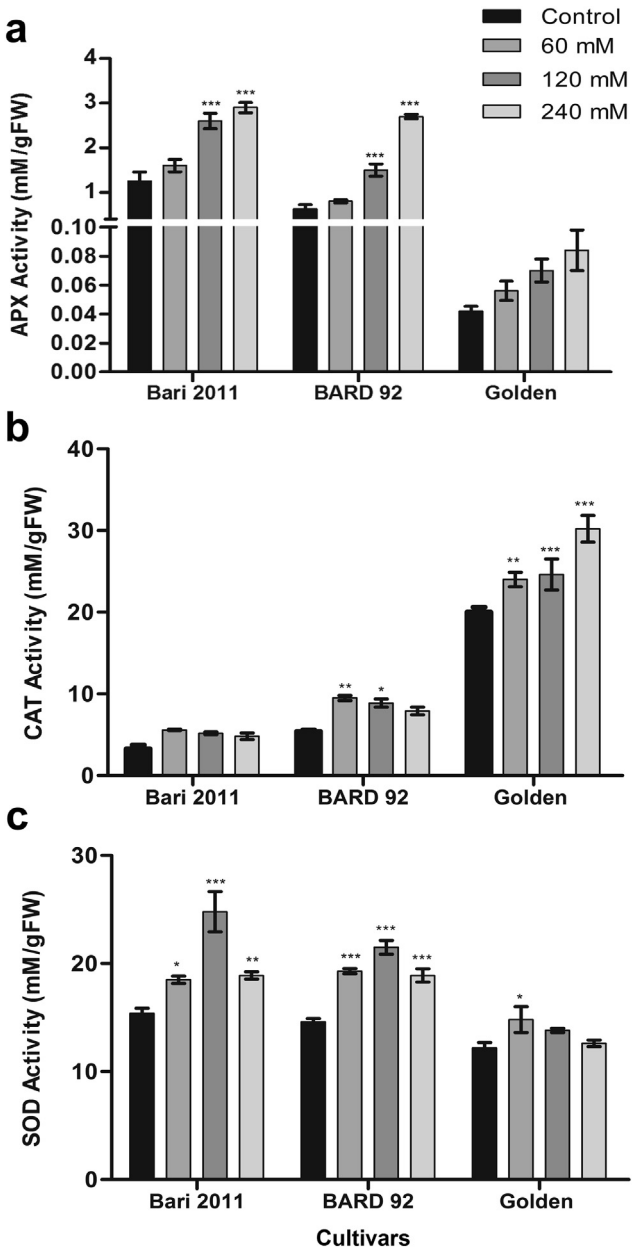

Fig. 11. Activity of enzymes involved in the antioxidation in three cultivars of peanut (Bari 2011, BARD 92 and Golden) **a** Effect of salinity on Ascorbate peroxidase (APX) activity of peanut seedlings (Two-way ANOVA: Interaction *p*-value = < 0.0001, Column factor *p*-value = < 0.0001, Row factor *p*-value = < 0.0001) **b** Effect of salinity on Catalase (CAT) activity of peanut seedlings (Two-way ANOVA: Interaction *p*-value = < 0.0001, Column factor *p*-value = < 0.0001, Row factor *p*-value = < 0.0001) **c** Effect of salinity on Superoxide dismutase (SOD) activity of peanut seedlings (Two-way ANOVA: Interaction *p*-value = < 0.0001, Column factor *p*-value = < 0.0001, Row factor *p*-value = < 0.0001). Data presented as mean ± S.E. *p*-value smaller than 0.05 is considered significant. '*' is depicting *p*-value<0.05, '**' *p*-value<0.01, '***' *p*-value<0.001.

value has been observed for any correlation which showed that AhFLS and AhLAR expression is not directly dependable on these selected parameters, but higher Pearson r value depicted some level of dependency. Differential expression of AhFLS and AhLAR along with accumulation pattern of flavonols and proanthocyanidins in all three selected cultivars at various salt concentrations indicated vital role of flavonols and proanthocyanidins in salt tolerance. Such differential expression indicated the presence of precise regularity molecular mechanisms that are yet to explored.

5. Conclusion

Over the course of time, plants have adapted themselves to the flatulating environmental conditions by engineering their metabolic pathways. Detailed understanding of metabolic enzymes can assist in the metabolic engineering of such pathways to produce stress tolerant varieties and production of desirable metabolites. Flavonols and proanthocyanidins are specific targets for metabolic engineering owing to their significant role in plant stress response and biological activities. The characterization of *AhFLS* and *AhLAR* given in this study could be a potential source for understanding the structure, function and regulation of these enzymes under stress. Furthermore, the present study would assist in the metabolic engineering of flavonoid biosynthetic pathway to produce stress tolerant varieties and production of proanthocyanidins and flavonols at an industrial scale.

Ethics approval and consent to participate

Not applicable.

Consent for publication

Not applicable.

Availability of data and materials

The data and results of this study are represented in the enclosed table, figures and supplementary materials.

Funding

This research was supported by the Higher Education Commission (HEC), Pakistan and National University of Sciences and Technology (NUST), Pakistan.

Authors' contributions

RA, GK and SH conceived the project. All co-authors were involved in planning the experiments. GK, SH, JM, TI, and MK conducted the experiments and collected the data. GK, SH, HA, MK, FM and RA performed data analysis and drafting of the manuscript. RA, FM, AG and HA revised the final manuscript.

Declaration of Competing Interest

The authors declare that they have no known competing financial interests or personal relationships that could have appeared to influence the work reported in this paper.

Acknowledgments

We extend our gratitude to Higher Education Commission (HEC), Islamabad, Pakistan for providing funding, National University of Sciences and Technology (NUST), Islamabad, Pakistan for providing research facilities, National Institute of Lasers and Optronics (NILOP), Islamabad, Pakistan for helping in fluorescence spectroscopy and National Agriculture Research Center (NARC), Islamabad, Pakistan for providing germplasm. We would like to acknowledge Mark E. Sorrells, Professor of Plant Breeding, Cornell University, NY,USA, for reviewing the manuscript.

Appendix A. Supplementary data

Supplementary data to this article can be found online at https://doi.org/10.1016/j.sjbs.2021.01.024.

References

Aebi, H., 1984. Catalase in vitro. Methods in Enzymology, Elsevier (USA).

Ali, H., Muhammad, S., Anser, M.R., Khan, S., Ullah, R., Muhammad, B., 2018. Validation of fluorescence spectroscopy to detect adulteration of edible oil in extra virgin olive oil by applying chemometrics 0003702818768485 Appl. Spectrosc.

Andersen, O.M., Markham, K.R., 2005. Flavonoids: Chemistry, Biochemistry and Applications. CRC Press.

Asiri, A.M., Marwani, H.M., Alamry, K.A., Al-Amoudi, M.S., Khan, S.A., El-Daly, S.A., 2014. Green synthesis, characterization, photophysical and electrochemical properties of bis-chalcones. Int. J. Electrochem. Sci. 9, 799–809.

Beauchamp, C., Fridovich, I., 1971. Superoxide dismutase: improved assays and an assay applicable to acrylamide gels. Anal. Biochem. 44, 276–287.

Bertioli, D.J., Cannon, S.B., Froenicke, L., Huang, G., Farmer, A.D., Cannon, E.K., Liu, X., Gao, D., Clevenger, J., Dash, S., 2015. The genome sequences of Arachis duranensis and Arachis ipaensis, the diploid ancestors of cultivated peanut. Nature Genet. 47, 438.

Bradford, M.M., 1976. A rapid and sensitive method for the quantitation of microgram quantities of protein utilizing the principle of protein-dye binding. Anal. Biochem. 72, 248–254.

Buer, C.S., Muday, G.K., Djordjevic, M.A., 2007. Flavonoids are differentially taken up and transported long distances in Arabidopsis. Plant Physiol. 145, 478–490.

Chavan, P.D., Karadge, B., 1980. Influence of salinity on mineral nutrition of peanut (Arachis hypogea L.). Plant Soil 54, 5–13.

Condat, M., Babinot, J., Tomane, S., Malval, J.-P., Kang, I.-K., Spillebout, F., Mazeran, P.-E., Lalevée, J., Andalloussi, S.A., Versace, D.-L., 2016. Development of photoactivable glycerol-based coatings containing quercetin for antibacterial applications. RSC Adv. 6, 18235–18245.

De Rijke, E., Joshi, H.C., Sanderse, H.R., Ariese, F., Udo, A., Gooijer, C., 2002. Natively fluorescent isoflavones exhibiting anomalous Stokes' shifts. Anal. Chim. Acta 468, 3–11.

Demirkaya-Miloglu, F., Kadioglu, Y., Senol, O., Yaman, M., 2013. Spectrofluorimetric determination of α-tocopherol in capsules and human plasma. Indian J Pharm. Sci 75, 563.

Djordjevic, M., Mathesius, U., Arioli, T., Weinman, J., Gärtner, E., 1997. Chalcone synthase gene expression in transgenic subterranean clover correlates with localised accumulation of flavonoids. Funct. Plant Biol. 24, 119–132.

Donaldson, L., Williams, N., 2018. Imaging and Spectroscopy of Natural Fluorophores in Pine Needles. Plants 7, 10.

Drabent, R., Pliszka, B., Olszewska, T., 1999. Fluorescence properties of plant anthocyanin pigments. I. Fluorescence of anthocyanins in Brassica oleracea L. extracts. Photochem. Photobiol. B. 50, 53–58.

Dubois, M., Gilles, K.A., Hamilton, J.K., Rebers, P.T., Smith, F., 1956. Colorimetric method for determination of sugars and related substances. Anal. Chem. 28, 350–356.

Elavarthi, S., Martin, B., 2010. Spectrophotometric assays for antioxidant enzymes in plants. Plant Stress Tolerance, Springer (USA).

Figueiras, T.S., Neves-Petersen, M.T., Petersen, S.B., 2011. Activation energy of light induced isomerization of resveratrol. J Fluoresc 21, 1897–1906.

Gasteiger, E., Hoogland, C., Gattiker, A., Wilkins, M.R., Appel, R.D., Bairoch, A., 2005. Protein identification and analysis tools on the ExPASy server. The proteomics protocols handbook, Springer (USA).

Guharay, J., Sengupta, B., Sengupta, P., 2001. Protein–flavonol interaction: fluorescence spectroscopic study. Proteins 43, 75–81.

Höfener, S., Kooijman, P.C., Groen, J., Ariese, F., Visscher, L., 2013. Fluorescence behavior of (selected) flavonols: a combined experimental and computational study. Phys. Chem. Chem. Phys. 15, 12572–12581.

Holser, R.A., 2014. Near-infrared analysis of peanut seed skins for catechins. Am. J. Analyt. Chem. 5, 378.

Horton, P., Park, K.-J., Obayashi, T., Fujita, N., Harada, H., Adams-Collier, C., Nakai, K., 2007. WoLF PSORT: protein localization predictor. Nucleic Acids Res. 35, W585–W587.

Hou, M., Zhang, Y., Mu, G., Cui, S., Yang, X., Liu, L., 2020. Molecular cloning and expression characterization of flavonol synthase genes in peanut (Arachis hypogaea). Sci Rep 10, 1–11.

Jaakola, L., Pirttilä, A.M., Halonen, M., Hohtola, A., 2001. Isolation of high quality RNA from bilberry (Vaccinium myrtillus L.) fruit. Mol. Biotechnol. 19, 201–203.

Jia, L.-G., Sheng, Z.-W., Xu, W.-F., Li, Y.-X., Liu, Y.-G., Xia, Y.-J., Zhang, J.-H., 2012. Modulation of anti-oxidation ability by proanthocyanidins during germination of Arabidopsis thaliana seeds. Mol Plant 5, 472–481.

Kearse, M., Moir, R., Wilson, A., Stones-Havas, S., Cheung, M., Sturrock, S., Buxton, S., Cooper, A., Markowitz, S., Duran, C., 2012. Geneious Basic: an integrated and extendable desktop software platform for the organization and analysis of sequence data. Bioinformatics 28, 1647–1649.

Lescot, M., Déhais, P., Thijs, G., Marchal, K., Moreau, Y., Van De Peer, Y., Rouzé, P., Rombauts, S., 2002. PlantCARE, a database of plant cis-acting regulatory elements and a portal to tools for in silico analysis of promoter sequences. Nucleic Acids Res. 30, 325–327.

Lichtenthaler, H.K., 1987. Chlorophylls and carotenoids: pigments of photosynthetic biomembranes. Methods in Enzymology. Elsevier, USA.

Livak, K.J., Schmittgen, T.D., 2001. Analysis of relative gene expression data using real-time quantitative PCR and the 2− ΔΔCT method. Methods 25, 402–408.

Lopez, F., Barclay, G., 2017. Plant Anatomy and Physiology. PharmacognosyElsevier, USA.

Martinez, V., Mestre, T.C., Rubio, F., Girones-Vilaplana, A., Moreno, D.A., Mittler, R., Rivero, R.M., 2016. Accumulation of Flavonols over Hydroxycinnamic Acids Favors Oxidative Damage Protection under Abiotic Stress. Front. Plant Sci. 7.

Maugé, C., Granier, T., D'estaintot, B. L., Gargouri, M., Manigand, C., Schmitter, J.-M., Chaudière, J., Gallois, B., 2010. Crystal structure and catalytic mechanism of Leucoanthocyanidin reductase from Vitis vinifera. J. Mol. Biol., 397, 1079–1091.

Morris, A.C., Djordjevic, M.A., 2006. The Rhizobium leguminosarum biovar trifolii ANU794 induces novel developmental responses on the subterranean clover cultivar Woogenellup. Mol. Plant Microbe Interact. 19, 471–479.

Muhlemann, J.K., Younts, T.L., Muday, G.K., 2018. Flavonols control pollen tube growth and integrity by regulating ROS homeostasis during high-temperature stress. Proc. Natl. Acad. Sci. UAS 115, E11188–E11197.

Nabavi, S.M., Šamec, D., Tomczyk, M., Milella, L., Russo, D., Habtemariam, S., Suntar, I., Rastrelli, L., Daglia, M., Xiao, J., 2018. Flavonoid biosynthetic pathways in plants: Versatile targets for metabolic engineering. Biotechnol. Adv.

Nabavi, S.M., Šamec, D., Tomczyk, M., Milella, L., Russo, D., Habtemariam, S., Suntar, I., Rastrelli, L., Daglia, M., Xiao, J., 2020. Flavonoid biosynthetic pathways in plants: Versatile targets for metabolic engineering. Biotechnol. Adv. 38.

Naeem-Ud-Din, M.T., Naeem, M., Hassan, M., Rabbani, G., Mahmood, A., Iqbal, M., 2012. Development of Bari-2011: A high yielding, drought tolerant variety of groundnut (Arachis hypogaea L.) with 3–4 seeded pods. J. Anim. Plant Sci. 22, 120–125.

Nakano, Y., Asada, K., 1981. Hydrogen peroxide is scavenged by ascorbate-specific peroxidase in spinach chloroplasts. Plant Cell Physiol. 22, 867–880.

Ngaki, M.N., Louie, G.V., Philippe, R.N., Manning, G., Pojer, F., Bowman, M.E., Li, L., Larsen, E., Wurtele, E.S., Noel, J.P., 2012. Evolution of the chalcone-isomerase fold from fatty-acid binding to stereospecific catalysis. Nature 485, 530–533.

Pal, S., Saha, C., Hossain, M., Dey, S.K., Kumar, G.S., 2012. Influence of galloyl moiety in interaction of epicatechin with bovine serum albumin: a spectroscopic and thermodynamic characterization. PLoS One 7.

Park, H.-R., Daun, Y., Park, J.K., Bark, K.-M., 2013. Spectroscopic properties of flavonoids in various aqueous-organic solvent mixtures. Bull. Korean Chem. Soc. 34, 211–220.

Peer, W.A., Brown, D.E., Tague, B.W., Muday, G.K., Taiz, L., Murphy, A.S., 2001. Flavonoid accumulation patterns of transparent testa mutants of Arabidopsis. Plant Physiol. 126, 536–548.

Pelletier, M.K., Murrell, J.R., Shirley, B.W., 1997. Characterization of flavonol synthase and leucoanthocyanidin dioxygenase genes in Arabidopsis (Further evidence for differential regulation of" early" and" late" genes). Plant Physiol. 113, 1437–1445.

Pokhrel, L.R., Dubey, B., 2013. Evaluation of developmental responses of two crop plants exposed to silver and zinc oxide nanoparticles. Sci. Total Environ. 452, 321–332.

Rausher, M.D., Miller, R.E., Tiffin, P., 1999. Patterns of evolutionary rate variation among genes of the anthocyanin biosynthetic pathway. Mol. Biol. Evol. 16, 266–274.

Rauter, A.P., Ennis, M., Hellwich, K.-H., Herold, B.J., Horton, D., Moss, G.P., Schomburg, I., 2018. Nomenclature of flavonoids (IUPAC Recommendations 2017). Pure Appl. Chem. 90, 1429–1486.

Saeed, I., Hassan, M.F., 2009. High yielding groundnut (Arachis hypogea L.) variety "Golden". J. Pak J. Bot. 41, 2217–2222.

Saito, K., Yonekura-Sakakibara, K., Nakabayashi, R., Higashi, Y., Yamazaki, M., Tohge, T., Fernie, A.R., Biochemistry 2013. The flavonoid biosynthetic pathway in Arabidopsis: structural and genetic diversity. J. Plant Physiol., 72, 21–34.

Schwede, T., Kopp, J., Guex, N., Peitsch, M.C., 2003. SWISS-MODEL: an automated protein homology-modeling server. Nucleic Acids Res. 31, 3381–3385.

Singh, V., Mishra, A.K., 2015. White light emission from vegetable extracts. Sci. Rep. 5, 11118.

Tu, L.-Y., Pi, J., Jin, H., Cai, J.-Y., Deng, S.-P., 2016. Synthesis, characterization and anticancer activity of kaempferol-zinc (II) complex. Bioorg. Med. Chem. Lett. 26, 2730–2734.

Voicescu, M., Ionescu, S., Gatea, F., 2014. Photophysical properties of some flavones probes in homogeneous media. J. Fluoresc. 24, 75–83.

Weber, G., Teale, F., 1957. Determination of the absolute quantum yield of fluorescent solutions. J. Chem. Soc. Faraday Trans. 53, 646–655.

Xu, H., Li, Y., Tang, H.-W., Liu, C.-M., Wu, Q.-S., 2010. Determination of rutin with UV-Vis spectrophotometric and laser-induced fluorimetric detections using a non-scanning spectrometer. Anal. Lett. 43, 893–904.

Yonekura-Sakakibara, K., Higashi, Y., Nakabayashi, R., 2019. The origin and evolution of plant flavonoid metabolism. Front. Plant Sci. 10, 943.

Zhang, L., Wang, P., Ma, X., Zhao, W., Li, M., Yao, S., Liu, Y., Gao, L., Xia, T., 2020. Exploration of the Substrate Diversity of Leucoanthocyanidin Reductases. J. Agric. Food Chem. 68, 3903–3911.

Zhang, Z., Huang, R., 2013. Analysis of malondialdehyde, chlorophyll proline, soluble sugar, and glutathione content in Arabidopsis seedling. Bio Protoc. 3.